Investigations on the Oxide Removal Mechanism during Ultrasonic Wedge-Wedge Bonding Process

Yangyang Long[1], Folke Dencker[2], Friedrich Schneider[3], Benjamin Emde[3], Chun Li[1]
Jörg Hermsdorf[3], Marc Wurz[2], Jens Twiefel[1]
[1]Institute of Dynamics and Vibration Research, Leibniz Universität Hannover
Appelstr. 11, 30167 Hannover, Germany
[2]Institute of Micro Production Technology, Leibniz Universität Hannover
An der Universität 2, 30823 Garbson, Germany
[3]Laser Zentrum Hannover e.V.
Hollerithallee 8, 30419 Hannover, Germany
Ph: +49 511-762-17558; Fax: +49 511-762-4164
Email: long@ids.uni-hannover.de

Abstract

As an inevitable step during ultrasonic bonding of aluminum or copper materials, the removal of oxides that prevent the bond formation is essential for obtaining high quality. Nevertheless, the oxides removal process is still unclear after tens of years' application of ultrasonic bonding. In this project, the removal mechanism was investigated via the analysis of an artificially coated oxide layer. The oxide removal process was observed in real-time by a high-speed observation system and the oxides distribution after the bonding process was observed under an electron microscope. The results show that during the bonding process, the detached oxides first agglomerate into larger particles and were then pressed outside of the contact area. The areas of the particles were counted and fit to a lognormal distribution.

Introduction

Ultrasonic (US) wire bonding has been dominating the interconnection market within microelectronic packaging industry for decades. Trillions of wires are yearly bonded and it cannot be replaced by any other technique in the coming tens of years [1]. Due to its high speed, short process time and tiny dimensions, however, there are still many gaps towards a better understanding of the complicated phenomena taking place at the two interfaces within the bonding domain - the wire/substrate interface and the wire/tool interface. Among these phenomena, the removal of oxide from the contact interface is essential to the bonding process and need more investigations.

In general, the removal of the oxide layer during the bonding process consists of three stages: 1) segmentation of the oxide layer; 2) detachment of the segmented oxide particles; 3) transportation of the detached oxide particles. Aluminum oxide on commonly used aluminum wire or substrate is very brittle and cracks occur during the loading of the normal force, especially at the peripheral region of the contact surface [2]. Apart from this, the tips of asperities induce cracks to the oxide on the counter surfaces [3]. The US vibration and the material flow induced by plastic deformation lead to the detachment of the oxide particles from pure metal surfaces. Most of the oxide particles are then propelled to the outside of the contact interface. The rest of the particles get trapped into the valleys among asperities [4,5].

The way the oxide particles are transported to the peripheral region of the contact interface is still unknown to researchers even though it is well known that the US wedge-wedge bonding process has a very high self-cleaning efficiency. It has been demonstrated by Krzanowski and Murdeshwar [6] that a layer of 40 nm carbon contamination does not influence the bond strength. Maeda et al. [7] tried to analyze the oxides removal path underneath the wire. It was found that most oxide particles piled up at the periphery and some particles rolled like a snowball during the removal process. With regard to the wire/tool interface, almost no research has been conducted due to its lower importance compared to the wire/substrate interface. Nevertheless, the detection of adherence forces at the wire/tool interface indicates that some oxides at this contact interface were also removed during the bonding process. This is also in accordance to the existence of a relative motion between the wire and the tool [8,9].

The present project attempted to investigate the oxide removal mechanism via artificially coated wires. The oxide removal process was observed in real-time and the oxide particles were observed afterwards as well.

Experimental Setup

It has been proved in [8,9] that the relative motion between the wire and the tool behaves as a combination of micro-slip behavior and stick-slip behavior, which is similar to that between the wire and the substrate. As a result, the oxide removal processes at the two interfaces reveal similar information which leads to a better understanding of the removal mechanism. Due to the nano-scale of the oxide layer, it is extremely hard to directly observe the oxides. Therefore in the current project, the oxide layer on the surface of the wire was thickened by an artificial coating of aluminum oxide so that the analysis of the removal mechanism was easier.

A. Specimen

The aluminum wire Al-H11 from Heraeus GmbH was used in this project. The diameter of the wire is 400 µm and it has a breaking load of 500~700 cN and more than 5% elongation. The same as a pure aluminum material, a natural oxide layer with an average thickness of 5 nm covers the wire.

Some of the wires were mounted on a frame as shown in Fig. 1 and then coated within a Kenotec RF (13.56 MHz) 6.5'' target magnetron sputter device. The wires were mounted on an aluminum frame and coated from two sides to achieve a homogenous coverage on the whole wire surface. Different amounts of Al_2O_3 were deposited to achieve different thicknesses of oxide layers (50 and 200 nm) in order to

978-1-5090-4369-9/16/$31.00 ©2016 IEEE

compare the influence of the thickness on the removal process. The following parameters were used for coating:

Al_2O_3: 500 W, 95 sccm Ar, 5 sccm O_2, 5 x 10^{-3} torr with a deposition rate of 6 nm/min.

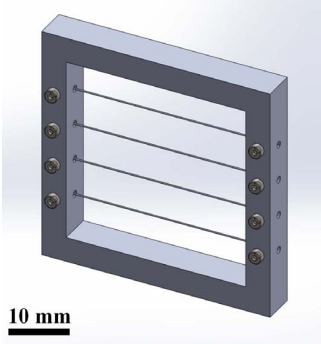

Fig. 1 Mounting frame for wire coating

To prevent material property changes of the wire, the coating process was conducted iteratively so that the substrate temperature was not high. The sputtering process was interrupted every 10 min followed by a 5 min break for cooling.

Finally, three specimens were prepared:

1) Al-H11 wire with 50 nm Al_2O_3 coating;
2) Al-H11 wire with 200 nm Al_2O_3 coating;
3) Al-H11 wire as received

B. Ultrasonic Bonding

The bonding head BJ910 from Hesse GmbH was used for wire bonding in the project. The bonding head ran at its natural frequency close to 60 kHz and was driven by an in-house developed digital phase controller [10] with the Brüel & Kjær 2713 amplifier. Pure aluminum plates were used as the bonding substrate.

The bonding normal force was set as 9 N while the input US power varied from 18~25 W. The bonding processes for all specimens lasted for 50 ms.

C. Real-time Observation

The oxide removal process was observed by a high speed observation system that consists of a high speed camera and a magnification system. The high speed camera Phantom v710 was received from Vision Research Inc. The CMOS sensor has a pixel size of 20 x 20 µm. A trade-off between the window size and the frame rate has been made to record the removal process. The window size used was 512 x 384 and the frame rate was 30,008 fps. The frame rate was about a half of the bonding frequency, but was able to record the removal process. The sharpness of the videos was confirmed by an exposure time of 2 µs. Due to the relatively large pixel size of the sensor, a reverse lens technique was applied to magnify the resolution. With a C-Mount 12.5 mm Pentax lens, a final resolution of 1.1 µm/pixel was reached. The setup together with the bonding platform is shown in Fig. 2.

To provide enough light onto such a tiny area (563.2 X 422.4 mm) within 2 µs, a laser source JOLD-45-CPXF-1P from Jenoptik AG was applied. The laser has a max power of 45 W and a wavelength of 804 to 808 nm depending on the applied power and temperature. The real-time observation experiments were performed within an aluminum box for protection.

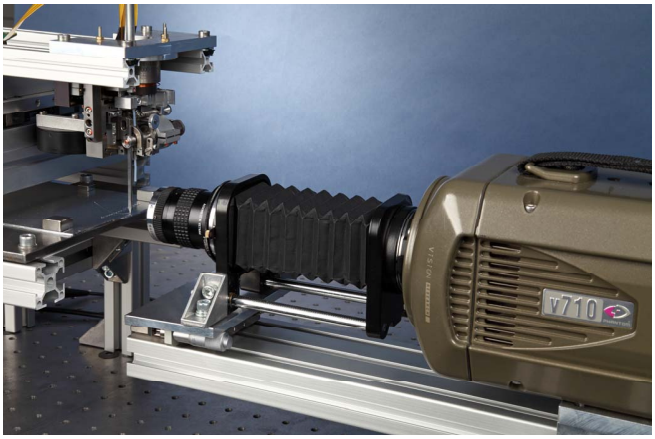

Fig. 2 Real-time observation of the US bonding process

D. SEM Observation

After the bonding process, the bonding specimens were taken to a scanning electron microscope (SEM) for post observation. A Zeiss LEO 1455 VP equipped with a secondary electron detector, a four quadrant backscattered electron detector and an EDAX 10 mm² energy dispersive spectrometry (EDS) detector was used. The shapes and distributions of oxide particles were analyzed.

Results and Discussion

A. Removal Process of Specimen 1

The first specimen was bonded onto an aluminum plate with an US power of ~22 W, which means the wire was over-bonded so that the removal process was enhanced. The whole bonding process was recorded by the real-time observation system.

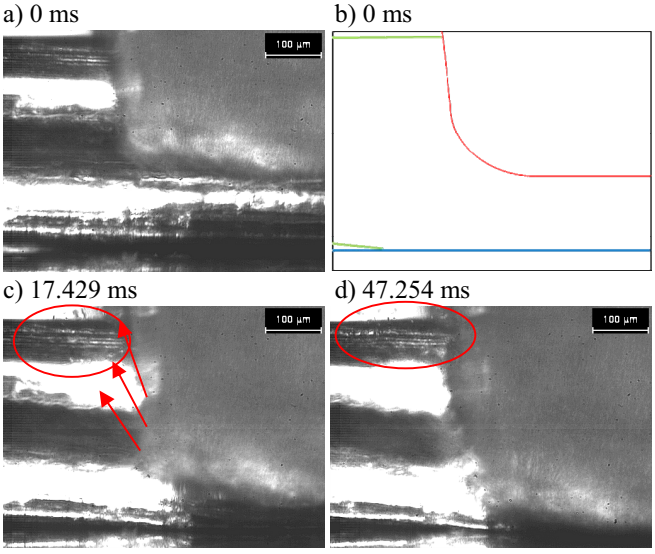

Fig. 3 Removal process on Al-H11 with 50 nm Al_2O_3

A series of images subtracted from the video are shown in Fig. 3. The initial state of the wire after the loading of the normal force is shown Fig. 3 a). The lines in b) display the boundaries of wire (in red), substrate (in blue) and wire (in green).

At about 1.366 ms, a particle flying outside of the wire/tool interface was observed. Afterwards, more and more particles were propelled outside of the contact interface and most of the particles flew to the upper-left which is noted by the arrows in Fig. 3 c). The amount of particles within the red circles remains more or less constant from about 10 ms until the end of the process, as seen in c) and d). The particles' sizes vary but are in micro-size, which indicates that the oxide particles first agglomerate together into larger particles during the transportation process within the contact interface.

As the particles were found to fly upwards, the bonding process was recorded with another window position which is above the wire/substrate interface as shown in Fig. 4 a) and b). The wire was below the green line while the tool was on the right-hand side of the red line.

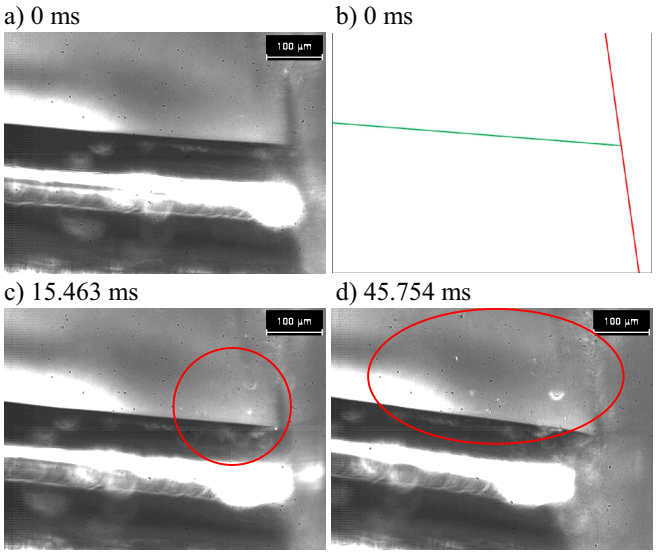

Fig. 4 Removal process on Al-H11 with 50 nm Al_2O_3 with a higher recording window position

In the beginning, the particles can only be observed at the corner between the wire and the tool as circled in Fig. 4 c). Again most particles were emitted to the upper-left direction. After about 20 ms, particles spread out in the space of the window as in Fig. 4 d). This continued to the end.

B. Removal Process of Specimen 2 and 3

Specimen 2 which was coated by 200 nm Al_2O_3 was used to compare the influence of the thickness. The bonding process for Specimen 2 was recorded with the window position above the wire/substrate interface. Two images from the video were shown in Fig. 5. By comparing the two videos, no significant difference between the removal processes of Specimens 1 and 2 were observed. This indicates that the influence of the thickness of the artificial oxide layer in this range (50~200 nm) can be neglected.

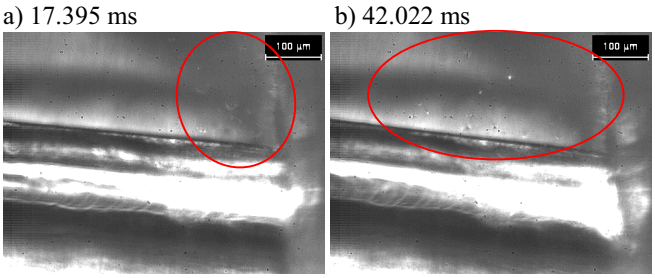

Fig. 5 Removal process on Al-H11 with 200 nm Al_2O_3

It must be noted that the artificial coated layer influences the relative motion behavior at the wire/tool interface. In this case, Specimen 3 was used to show whether a similar removal process takes place for the natural oxide layer. As the natural oxide layer was assumed to not show an obvious removal process as the above, the window position was moved to below the wire/substrate interface. Furthermore, the US power was increased to 25 W.

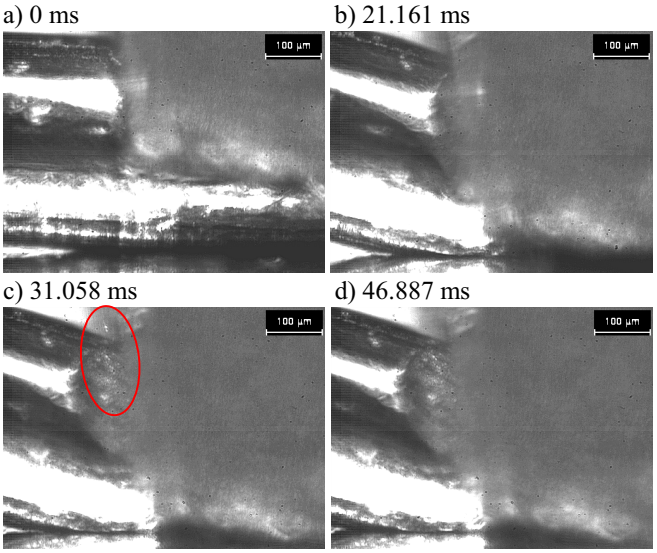

Fig. 6 Removal process on Al-H11

Although the same as expected, no particle emission was observed even when the wire was over-deformed as in Fig. 6 b). After about 21 ms, particles started to fly out. While after about 43 ms, no more particles were emitted. This indicates that for a normal wire bonding process, the detached oxide particles also agglomerate into larger particles. These large particles, however, will get trapped within the contact boundaries.

For nearly all of the specimens which were over-bonded with a high US power, an adherence force between the tool and the wire can always be detected. This indicated that the oxides on certain areas were removed so that microwelds could be formed.

C. Removal Process with Backlight

To record the removal process at the wire/substrate interface, a backlight is required. Since the laser source used

in the project is quite strong, a flat aluminum surface was placed at the back side of the bonding site to reflect the laser beam so that the sensor of the camera can be protected.

As shown in Fig. 7 a) and b), the part below the blue line is the substrate and the part on the right-hand side of the green line is the wire. The dark part below the blue line is the reflection of the wire due to the mirror effect of the aluminum substrate.

a) 0ms b) 0ms

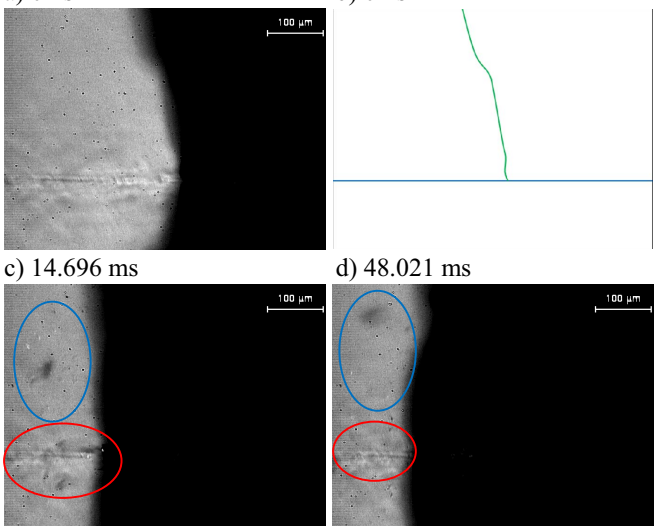

c) 14.696 ms d) 48.021 ms

Fig. 7 Removal process on Al-H11 with 200 nm Al2O3 at wire/substrate interface

In the beginning of the process, some particles were observed to hit the aluminum mirror and this gives a hint on the emission direction of some oxide particles. Many particles were observed to be emitted from the wire/substrate interface as those in the red circle in Fig. 7 c). More particles fell down from the upper side as in the blue circle in Fig. 7 d) due to the removal process at the wire/tool interface. This also proves that the removal processes at both interfaces are similar.

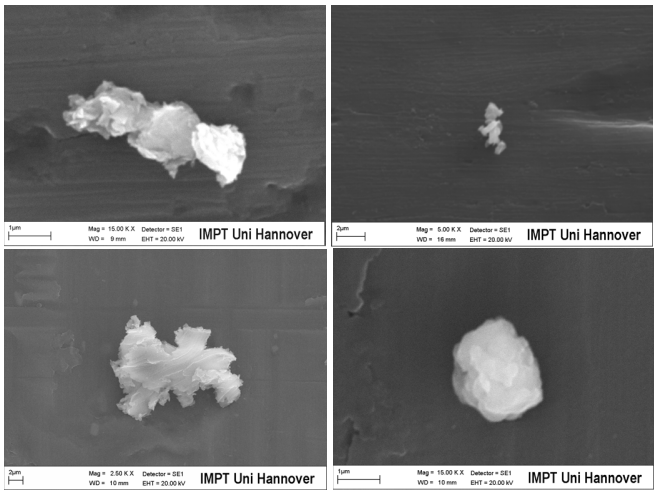

Fig. 8 Different oxide particles after the bonding process

a) Particles on Al-H11 with 50 nm Al_2O_3 after bonding

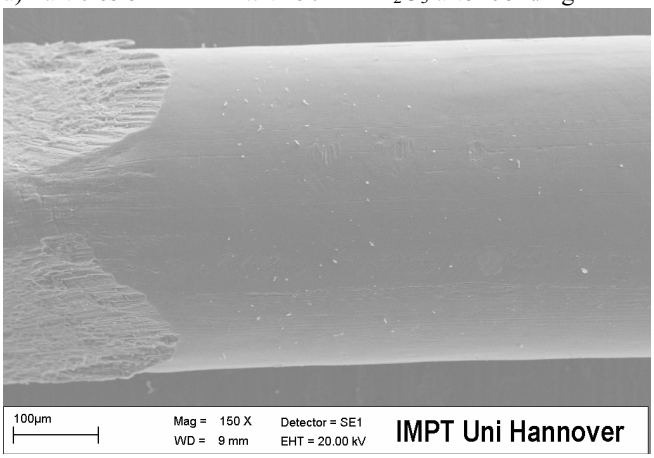

b) Display of only particles from a)

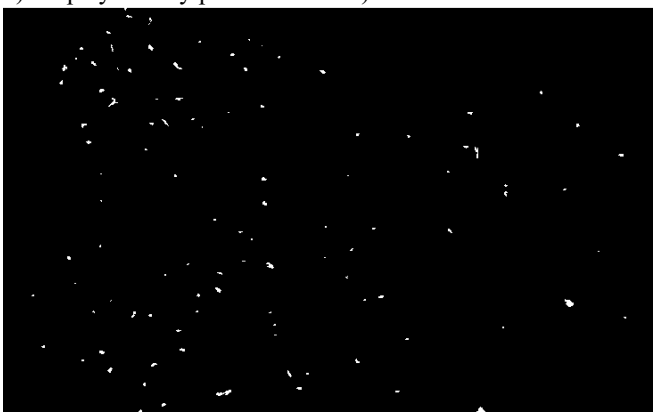

c) Particles on another Al-H11 with 50 nm Al_2O_3 after bonding

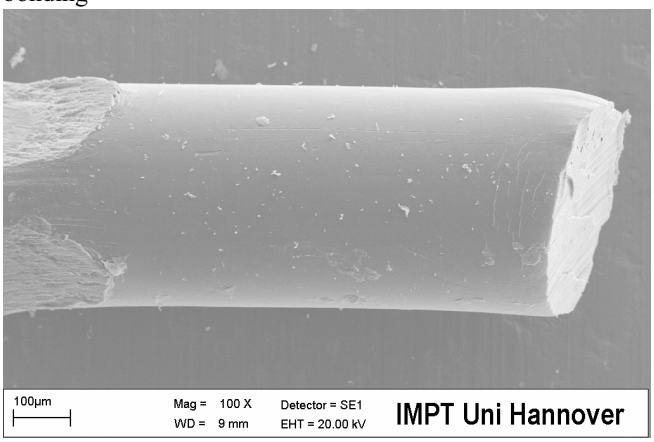

d) Display of only particles from c)

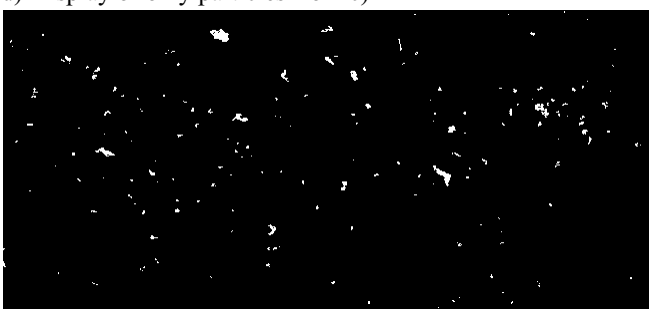

Fig. 9 The distribution of oxide particles

After the bonding processes, the bonded wires were mechanically removed to expose the wire/substrate interface. It was found that in most cases the whole interface was bonded, which means both the coated oxide and the natural oxide were removed during the 50 ms bonding process. This shows the high self-cleaning efficiency of the US wedge-wedge bonding process.

D. Distribution of Oxide Particles

After the bonding process, many oxide particles were found on the top surface of the wire. These particles have different shapes and sizes while all of them show a layered structure. Some particles from specimen 1) are chosen and shown in Fig. 8.

The distributions of the particles after the bonding process are shown in Fig. 9. It can be found that particles exist not only outside of the contact interface but also within the valleys of the contact surface. Some particles can be propelled a large distance of more than 1 mm from the border of the contact interface. Many particles were also found on the surface of the plate. Again, this proves that the wedge-wedge bonding process has a very high self-cleaning efficiency.

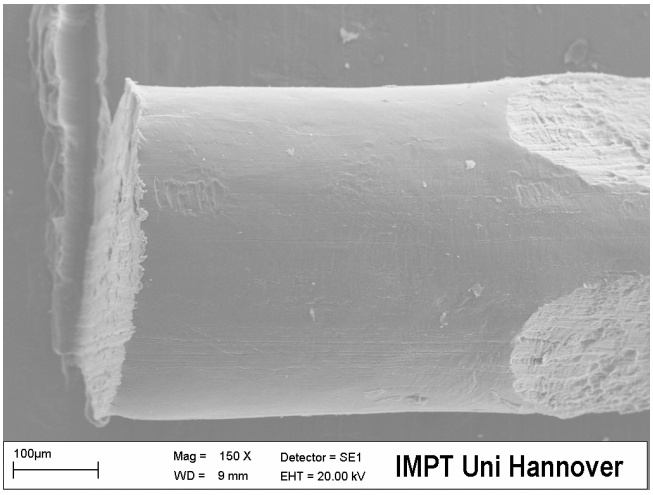

Fig. 10 Left-hand side of the specimen 1

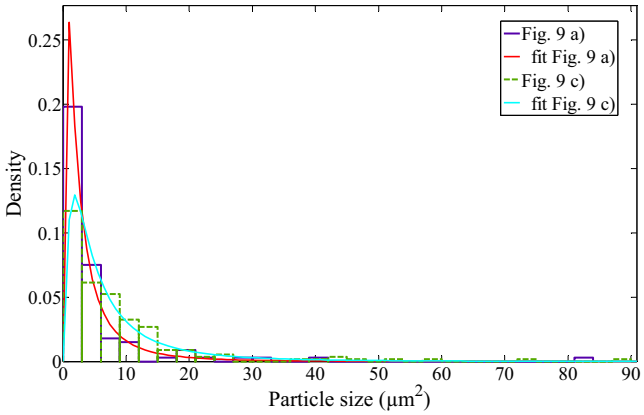

Fig. 11 The fitting of a lognormal distribution of particle areas

Compared to the right-hand side, fewer particles were found on the left-hand side of the specimen which is shown in Fig. 10. This might be due to the steeper surface of the wire (the region that contacts the smaller tool filet) that acts as an obstacle.

In order to count the areas of the particles, the SEM images were further processed with the MATLAB image processing tool. By selecting proper threshold values, only the oxide particles are now displayed. The corresponding processed images are shown in Fig. 9 b) and d).

Table 1 Lognormal distribution for particles in Fig. 9 a) and c)

Wire	µ	s	Mean
Fig. 9 a)	0.8828	1.1297	4.5765
Fig. 9 c)	1.6243	1.0385	8.7014

The areas of the particles were counted and statistically analyzed. The particles on both wires were found to fit lognormal distributions. The corresponding distribution parameters are shown in Table 1. A possible reason for the big difference between the mean values could be that the second wire got polluted. Some carbon contaminants have been recognized by the EDS test while not all contaminants could be excluded due to the large number of particles. In the near future, the influences of the bonding process on the particle size will be investigated.

Conclusions

The present project investigated an essential stage in US wire bonding process – the removal process of oxides which prevent bond formation. The results show that the wedge-wedge bonding has a very high self-cleaning efficiency (or serious friction) both at the wire/tool interface and the wire/substrate interface. The detached oxide particles first agglomerate into larger particles under the combined effect of continuous plastic deformation and vibration. Some of the larger particles are then transported to the outside of the contact interface while the rest of the particles stay within the contact surface. The particles that are emitted outside of the contact interface followed a lognormal distribution. The influence of the bonding process on the distribution will be further investigated.

Acknowledgments

We gratefully acknowledge the support from the Ministry of Science and Culture of Lower Saxony, Germany within the MARIO (Multifunktionale Aktive und Reaktive Interfaces und Oberflächen) program. Many thanks to Mr. Heiner Ramsbott from Vision Research Europe for his generosity of providing the lens.

References

1. Harman, G. G., Wire Bonding in Microelectronics, third ed., McGraw-Hill (New York, 2010).
2. Harman, G., Albers, J., "The ultrasonic welding mechanism as applied to aluminum-and gold-wire bonding in microelectronics," *IEEE Transactions on Parts, Hybrids, and Packaging,* Vol. 13, No. 4 (1977), pp. 406-412.

3. Seppänen, H., Kaskela, A., Mustonen, K., Oinonen, M., Haeggström, E., "Understanding Ultrasound-Induced Aluminum Oxide Breakage during Wire bonding," *IEEE International Ultrasonics Symposium*, New York, NY, Oct., 2007, pp. 1381-1384.
4. Geißler, U., Verbindungsbildung und Gefüge-entwicklung beim Ultraschall-Wedge-Wedge-Bonden von AlSi1-Draht, *Doctoral dissertation*, Technical University of Berlin, 2008.
5. Xu, H., Liu, C., Silberschmidt, V.V., Pramana, S.S., White, T.J., Chen, Z., "A re-examination of the mechanism of thermosonic copper ball bonding on aluminium metallization pads," *Scripta Materialia*, Vol. 61, No. 2 (2009), pp. 165-168.
6. Krzanowski, J. E., Murdeshwar, N., "Deformation and bonding processes in aluminum ultrasonic wire wedge bonding," *Journal of electronic materials*, Vol. 19, No. 9 (1990), pp. 919-928.
7. Maeda, M., Kitamori, S., Takahashi, Y., "Interfacial microstructure between thick aluminium wires and aluminium alloy pads formed by ultrasonic bonding," *Science and Technology of Welding and Joining*, Vol. 18, No. 2 (2013), pp. 103-107.
8. Long, Y., Twiefel, J., Roth, J., Wallaschek, J., "Real-Time Observation of Interface Relative Motion during Ultrasonic Wedge-Wedge Bonding Process," *48th International Symposium on Microelectronics*, Orlando, FL, Oct., 2015, pp. 000419-000424.
9. Long, Y., Dencker, F., Wurz, M., Feldhoff., A., Twiefel, J., "A deeper understanding on the motion behaviors of wire during ultrasonic wedge-wedge bonding process," *49th International Symposium on Microelectronics*, Pasadena, CA, Oct., 2016.
10. Ille, I., Twiefel, J., "Model-Based Feedback Control of an Ultrasonic Transducer for Ultrasonic Assisted Turning Using a Novel Digital Controller," *Physics Procedia*, vol. 70, 2015, pp. 63-67.